Civil Engineering Infrastructures Journal 2022, 55(2): 333-350
DOI: 10.22059/CEIJ.2021.325670.1761

RESEARCH PAPER

Assessment of Corrosion in Offshore R.C. Piers and Use of Microsilica to Reduce Corrosion Induced Oxidation (A Case Study of Wharves 11 and 12 in Imam Khomeini Port, Iran)

Tangtakabi, A.R.[1], Ramesht, M.H.[2*], Golsoorat Pahlaviani, A.[2] and Pourrostam, T.[2]

[1] Ph.D. Candidate, Department of Civil Engineering, Islamic Azad University, Central Tehran Branch, Tehran, Iran.
[2] Assistant Professor, Department of Civil Engineering, Islamic Azad University, Central Tehran Branch, Tehran, Iran.

Received: 16 Jun. 2021; Revised: 01 Nov 2021; Accepted: 09 Nov. 2021

ABSTRACT: Deterioration due to corrosion is an important issue affecting the durability, strength, and sustainability of buildings and structures. Many cities are located in coastal areas and many reinforced concrete structures in these areas are exposed to chloride aggressive marine environments. Therefore, it is important to provide protection and offer appropriate repair methods of buildings vulnerable to the degrading effects of corrosion. The present study sets out to identify and evaluate the causes and extent of corrosion observed in Piers 11 and 12 in Imam Khomeini port, Iran. The microsilica is used to reduce corrosion. In order to achieve the above-mentioned goals, a number of experimental field tests were performed to determine the level of concrete condition in terms of reinforcement corrosion. Some tests were conducted to determine the conditions of concrete piers in terms of reinforcement corrosion. Then a reinforcement corrosion current density test is performed using a potentiostat involving a placement process; with different water-to-cement ratios and superplasticizers, the microsilica content was 5%, 10%, and 15%. Microsilica can serve as an alternative to cement and was measured according to the ASTM standards. Microsilica was exposed to aggressive conditions at different periods and a concrete compressive strength test was performed. The results showed that the compressive strength and corrosion resistance of the concrete increased for concrete mixture containing 10% microsilica with a water-to-cement ratio of 34% and a superplasticizer ratio of 6%.

Keywords: Density, Imam Khomeini Port, Microsilica, Offshore Structures, Reinforcement Corrosion, Wharf.

1. Introduction

Concrete is one of the common engineering materials that have frequently been used over the last 100 years (Abedini and Zhang, 2021; Zhang et al., 2020). Experts have always considered this material to construct various structures such as buildings, piers, ports, tanks, bridges, and other various structures. Even today concrete is used on a

* Corresponding author E-mail: Mhramesht@yahoo.com

wide scale in modern societies, and will most probably be employed in future. The reason is that it shows excellent mechanical performance, has high durability, and is characterized by its low cost and energy consumption (He et al., 2020; Antunes et al., 2021). One of the most common causes of destruction in reinforced concrete structures is the deterioration of offshore concrete ones due to reinforcement corrosion under the influence of chloride ions.

In recent years, extensive researches have been conducted in this field, and corrosion has been dealt with as the most important phenomenon in discussions about the damage threatening concrete structures in an offshore environment. Of course, the existence of unfavorable conditions in these areas reveals the need for repairing the structure and determining their service life. From the point of view of armature corrosion in concrete structures, the conditions determining offshore structures on the margin of the Persian Gulf have turned this area into one of the most aggressive ones in terms of both solutes in seawater and their climatic conditions. So far, the concrete structures in the Persian Gulf have inflicted severe damage and high repair costs on the countries in the regions. This situation has come about through the corrosion of buried reinforcement, which is regarded as a serious economic problem. As a result, increasing attention has been paid to identifying the causes of reinforcement corrosion, preventing it, and tracing factors contributing to the highest strength and durability of concrete structures (Liu et al., 2021).

Parrott (1994) examined carbonation-induced corrosion and introduced the “un-neutralized remainder” measure, which is the difference between the concrete cover and the depth of carbonation. Corrosion was found to increase when the un-neutralized remainder approaches zero and becomes negative. However, corrosion halts, as this value approaches less than -10 mm. Roy et al. (1999) examined the reasons for corrosion as a product of humidity level. This process can be complex since maximum carbonation is obtained at 75% and 92% humidity. Besides, pore size is an important factor, with larger pores facilitating higher penetration and hence more corrosion. Furthermore, the rate of carbonation was shown to be directly proportional to the strength of concrete.

It is important to mention that the exposure of reinforced concrete structures to chemical and electrochemical damage is attributable to the phenomena of chloride infiltration (Zhang and Abedini, 2021) which is the most important cause of corrosion in this area. The useful life of the offshore concrete structures is significantly reduced due to reinforcement corrosion and concrete cracking. This type of damage is to be seen more in the tidal zone because the intensified penetration of chloride into the concrete in it is due to wetting and drying, and as a result, increases the corrosion current density (Liu et al., 2021). Moreover, concrete repair is one of the important aspects of the maintenance of concrete structures. On the other hand, the maintenance of concrete piers is considered to be one of the most important causes of the life span of concrete structures in the world, to which is allocated large sums of money every year.

Increasing the durability and the life span of these repairs provides an index of the selection of materials. Given that selecting suitable materials for repair has received attention in most parts of the world and, as a result, significant progress has been made in this field. However, this industry still suffers from shortcomings as far as concrete repairs are concerned. In this connection, recent studies of repairs to piers, bridge decks, and other structures have shown that the failure of a repair operation is due to various factors, including an improper selection of repair materials, low execution skills, and insufficient properties of primary concrete. This means that a good repair improves the performance of offshore structures or buildings. By contrast, poor

repair disables structure performance in a relatively short time. The reason is that the suitable choice of repair materials depends on their properties and the behavior of composite parts.

The performance of cement paste has already been investigated by adding microsilica (7% and 10% as cement substitute) to ordinary Portland cement Type 2 under wetting and drying conditions. The results show the excellent performance and higher strength of concrete containing microsilica, as against ordinary concrete, which does not use it. In addition, the results showed that capillary water uptake increased in those parts which were exposed to the tidal zone through using a larger amount of microsilica in the mixtures (Ganjian and Pouya, 2009). Bagheri et al. (2013) conducted a number of experiments and observed that concrete electrical resistivity could increase five times by replacing 12% microsilica with cement.

Pandey and Kumar (2019) performed an evaluation on the water absorption and chloride ion penetration of rice straw ash and microsilica admixed pavement quality concrete. They derived two equations for both initial and secondary rate of water absorption. Moffatt and Thomas (2018) showed that, given the same duration and conditions, the performance of concrete which contained fly ash and microsilica exposed to an offshore environment could decrease the depth of chloride penetration from 90 to 40 mm, as against all the control samples which had no fly ash or microsilica in them. Also, the results of permeability test indicate a significant increase resistance against chloride ion penetration for concrete containing fly ash and microsilica. In addition, the results of the test indicate a significant increase in resistance to chloride ion penetration in the case of concrete containing fly ash and microsilica. Siddique (2011) pointed out that the use of microsilica in concrete eliminates weak interfacial areas by strengthening the bond between cement paste and aggregates, and by forming structures with less porosity and more homogeneity. This has the effect of increasing the compressive strength of concrete. Based on what discussed above, one of the main objectives of this study is to assess the amount of corrosion seen in concrete piers mentioned above and determine the role of microsilica in increasing their compressive strength and reducing their corrosion.

2. Location of Case Study Offshore

The project site of the western Piers 11 and 12 is located in Imam Khomeini port in the southwest of Khuzestan province, and at the northeastern end of Khoor Mussa in the coastal areas of the Persian Gulf (see Figure 1).

Fig. 1. A satellite image of the wharves 11 and 12 at Imam Khomeini Port

In such areas, water and soil are polluted, and even the regional atmosphere contains elements which are harmful to the Persian Gulf. Moreover, in the areas under discussion, humidity and temperature are so high that they not only set off the process of structural destruction, but increase the speed of damage as well. Wharves 11 and 12 are important and strategic since they play a major role in accelerating the process of exporting and importing goods at the port in question, which has a total mooring length of about 1.5 km. These wharves were planned by the consultants of Iran Compsax in 1970. Having been designed and approved, their construction operations began in 1975 and ended in 1978.

3. Evaluating Offshore Concrete Structures

Appropriately repairing failures to extend the useful life of offshore concrete structures is indeed the best method whereby premature failures can be prevented. This means that such repair and reconstruction of structures entails high costs. Taking preventive measures can reduce, at least to some extent, the costs incurred. Moreover, periodic visits play a significant role in deciding on preventive action before any major damage is done. This has the advantage of reducing repair and reconstruction costs. Decisions can also be made about structural evaluation through occasional observation of faults. A periodic evaluation of structures is performed based on determining the need for maintenance, restoration, and reconstruction. This involves two stages of initial and final visits. The estimated type of fault and the penetration of chloride ions are the main agents of corrosion onset in reinforcement buried in concrete in most offshore structures (Babaee and Castel, 2016). It is, vital to study concrete resistance to chloride ion penetration. Such ions enter concrete both from an external environment by contact with contaminated soil or seawater and from an internal one using calcium chloride-based accelerated additives or contaminated materials containing ions. It must be emphasized that this is a well-known mechanism whereby chloride ions penetrate into the concrete, thus reducing the useful life of such structures (Babaee and Castel, 2018). Also noteworthy is the fact that the penetration of chloride ions into concrete is determined not by one, but rather by several factors (ionic release, capillary absorption, and suction, permeability, and migration) associated simultaneously with the environment which contains chloride ions (Bagheri et al., 2012). Tests are necessary to determine the exact type and number of faults for designing supplementary tests. After completing the structure evaluation, its service life was determined, and requisite decisions were made regarding the maintenance, repair, or reconstruction of the structure. Figure 2 shows the schematic chart of periodic inspection and evaluation cycle.

4. Evaluation Tests of Concrete Structures

Concrete evaluation tests are generally performed on non-destructive concrete to achieve the following objectives: 1) Preparing a chloride ion profile (chloride ion concentration and the amount of penetration into different depths of internal concrete) to determine the corrosion status in reinforcements; 2) Determining concrete electrical resistivity; 3) Determining the pulse speed and concrete mechanical modulus.

4.1. Preparing the Chloride Ion Penetration Profile

Penetration of chloride ions is the main agent of corrosion onset in reinforcements buried in concrete in most offshore structures. Therefore, it is of particular importance to study the concrete resistance to chloride ion penetration.

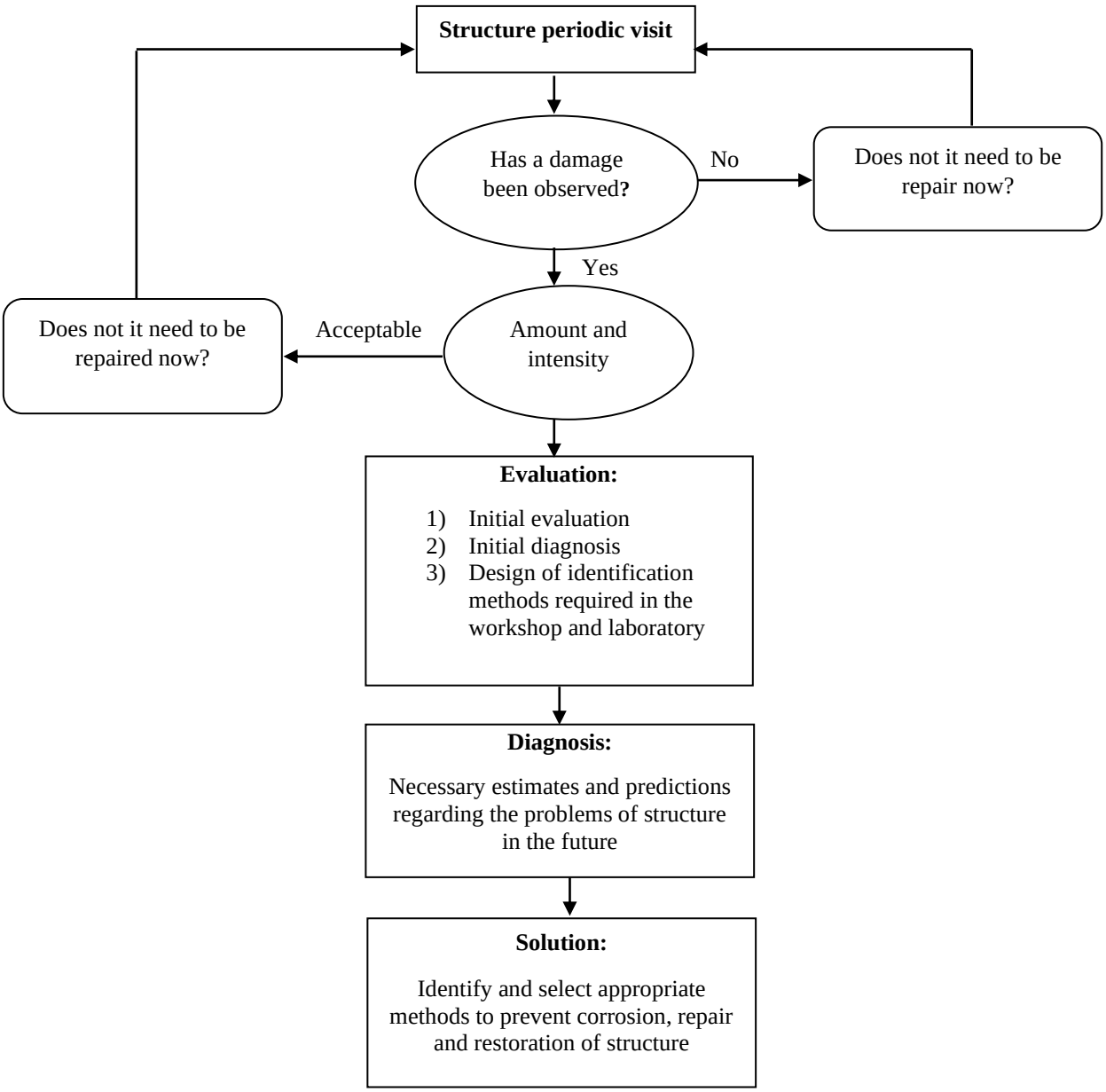

Fig. 2. The cycle of periodic evaluation and offshore concrete structures evaluation

Chloride ions enter into the concrete both from the outside environment, by contact with contaminated soil or seawater, and from the internal environment using calcium chloride-based accelerator additives or by using contaminated materials with chloride ions. It is well-known that the mechanisms of chloride ion penetration into concrete are due to the great importance of chloride ion penetration as an essential factor in reducing the useful life of concrete structures. Effects of corrosion on the properties of materials that result from the penetration of chloride ions include the deterioration of such properties (cover), limited concrete (core), longitudinal and transversal reinforcements, and connection between concrete and steel. The onset time of corrosion and corrosion surface (i.e., structure deterioration relating to the process of reinforcement corrosion) consists of three stages. The first stage is connected with diffusion, a process in which chloride ions disperse on enforcement surfaces. The second stage concerns the development from the onset time of corrosion until concrete begins to crack. The third stage has to do with

deterioration. This paper presents a model of chloride ion corrosion based on Fick's second law in order to simulate the theory and mathematics of the steps mentioned above. The concentration of concrete chloride is a function of depth and time according to Fick's second law and a one-dimensional solution based on developed models (Li and Zheng, 2005).

$$c(x,t) = cs[1 - \text{erf}\left(\frac{x}{2\sqrt{Dc * t}}\right)] \quad (1)$$

where *C(x,t)*: is the concrete chloride concentration, *cs*: is the surface chloride concentration, *Dc*: is the concrete chloride diffusion coefficient, *x*: is depth of concrete surface, *t*: is time and *erf*: is the error function.

When chloride concentration on the surface of the reinforcement reaches a critical level, reinforcement corrosion starts. Various functions have been introduced for critical chloride concentration, based on the existing environmental conditions. The function proposed for this study is connected with a particular region near the Persian Gulf. In this study, the onset time of corrosion has been proposed as a result of laboratory studies (base on the simulated environmental conditions prevailing in the Persian Gulf and the Oman Sea), and experimental studies of the true corrosive environmental conditions in southern regions of Iran have been done. This can be represented as follows:

$$Tcorr = 0.75\left(\frac{dc}{B1}\right)c1 \quad (2)$$

where $Tcorr$: is onset time of corrosion (years), and dc: is the thickness of steel bar coat (mm), c_1 and B_1: are fixed coefficients. It must be noted that the coefficients depend on the ratio of cement to water and the percentage of microsilica used in designing the concrete mix.

The diameter of reinforcement decreases over time as a result of corrosion. Eq. (3) is meant to calculate the reduction of the steel rod's corroded diameter based on the calculated corrosion onset. Thus:

$$db = dbi - 1.508\left(1 - \frac{w}{c}\right) - \frac{1.64}{dc}(t - Tcorr)0.71 \quad (3)$$

where d_b: is the reduced steel bar diameter, d_{bi}: is the initial diameter of steel bar, and *w/c*: is the water-cement ratio.

Based on the reduced diameter of the steel bar due to corrosion, the amount of corrosion ($\Delta corr$) in terms of reduction of the reinforcement diameter is defined as follows:

$$\Delta corr = \frac{d2b - d2bi}{d2bi} \times 100 \quad (4)$$

where $\Delta corr$: is the amount of corrosion, *d2b*: is the reduced steel bar diameter and *d2bi*: is the initial diameter of steel bar.

As can be verified, first the corrosion occurs on the bar, and then, owing to the expansion of the corrosion products, cracking takes place in the cover of concrete piers. Based on the preceding remarks, one of the most important tests for determining the quality of concrete is to prepare a penetration profile of chloride ions in the depth of concrete. For the purposes of this study, our tests were conducted by following the ASTM C1152 standard method, as explained below.

4.1.1. First Stage: Collection of Concrete Powder from the Structure

At least 10 grams of concrete powder taken from different depths of piers were required in order to draw chloride ion profiles. For this purpose, two methods were used (drilling and core extraction based on RILEM TC-178 method) and concrete powder was prepared in the laboratory. In the drilling method, a drill with an adjustable ruler was used to make a number of holes in the desired location according to the diameter of the drill. This involved 5 steps, during each of which a hole with a depth of one centimeter was

dug. The resulting concrete powder was stored and encoded bags to prevent any moisture. As for the core extraction method, first the sample of the cylinder was taken from the concrete held by a clamp. Then, the powder was prepared from the primary surface layer of each member by drilling a hole on the basis of the process described above. Finally, the samples were transferred to the laboratory, where steps were taken to prepare the solution by passing the powder through a 70-point sieve. It should be noted that an on-site drilling method was used at the pier (Figure 3).

4.1.2. Second Stage: Solution of Chloride Ion in Nitric Acid

The solution was prepared according to ASTM C114 (2017), Part 19. For this purpose, first, 10 grams of concrete powder was poured into Erlenmeyer, which passed through a 70-degree sieve. Then 75 ml of distilled water was poured into Erlenmeyer, and immediately afterwards nitric acid was diluted, drop by drop, with distilled water to a volume of 25 ml. This was added to a mixture of concrete and distilled water to dissolve all the chloride ions in acid. In order to ensure the dissolution of total chloride ions in acid, 2 to 3 drops of methyl orange index were poured into the solution. If the index rated the solution as acidic, all chloride ions were dissolved in the acid. Afterwards, the solution was heated to the boiling-point and passed through a filter paper. The volume of this solution, which contained distilled water, reached a level of 250 ml. Figure 4 illustrates all the steps involved.

4.1.3. Third Step: Determination of Chloride Ions Concentration in the Solution

To measure the amount of chloride ions in the solution, which used a tetrapetometric device because it was only needed to pour a certain amount of this solution into this device and specify its amount. The amount of chloride ions was determined in the solution, to divide the ions by 10 grams to measure their quantity, and to obtain their percentage. The solution was measured 3 times, and in different volumes, by the device. Then the weighted average was taken from the results in order to measure the amount of chloride ion in the solution. This was done to make the measurement as accurate as possible. The results were given as input to Excel software, which determined the average depth, and plotted the profile of chloride ion penetration.

4.2. Electrical Resistivity of Concrete

Determining concrete electrical resistivity is a suitable indicator whereby one can evaluate concrete permeability and its resistance to penetration of chloride ions and also concrete resistance to the passage of electric currents. In this connection, two anodic and cathodic regions are formed in the process of re-bar corrosion that are potentially different. This means that the transfer of hydroxyl ions from the cathode to the anode takes place under the influence of concrete electrical resistivity. For the higher electrical resistivity of the concrete lower's corrosion current density. What distinguishes this method is that it is quite non-destructive, and its simplicity, speed, and economy make it more efficient. Note that the ions which have penetrated into the concrete move through its pores, and that the concrete has electrical conductivity cause by the movement of ions. Of course, the amount of concrete electrical resistivity depends directly on its permeability and environmental conditions (the moisture of the concrete and the number of ions which have penetrated into it). There is no doubt that if concrete permeability is higher, ions can enter the concrete environment easily and quickly, and that if the number of penetrating ions is higher, concrete electrical resistivity will be less. Therefore, concretes with a high electrical resistivity will show better performance against penetration of chloride ion and the onset of corrosion. It is usually the case that chemical additives do not reduce the

electrical resistivity of concrete, but the effect of pozzolanic materials such as microsilica is significant since it increases such resistance.

Fig. 3. Concrete drilling to get concrete powder

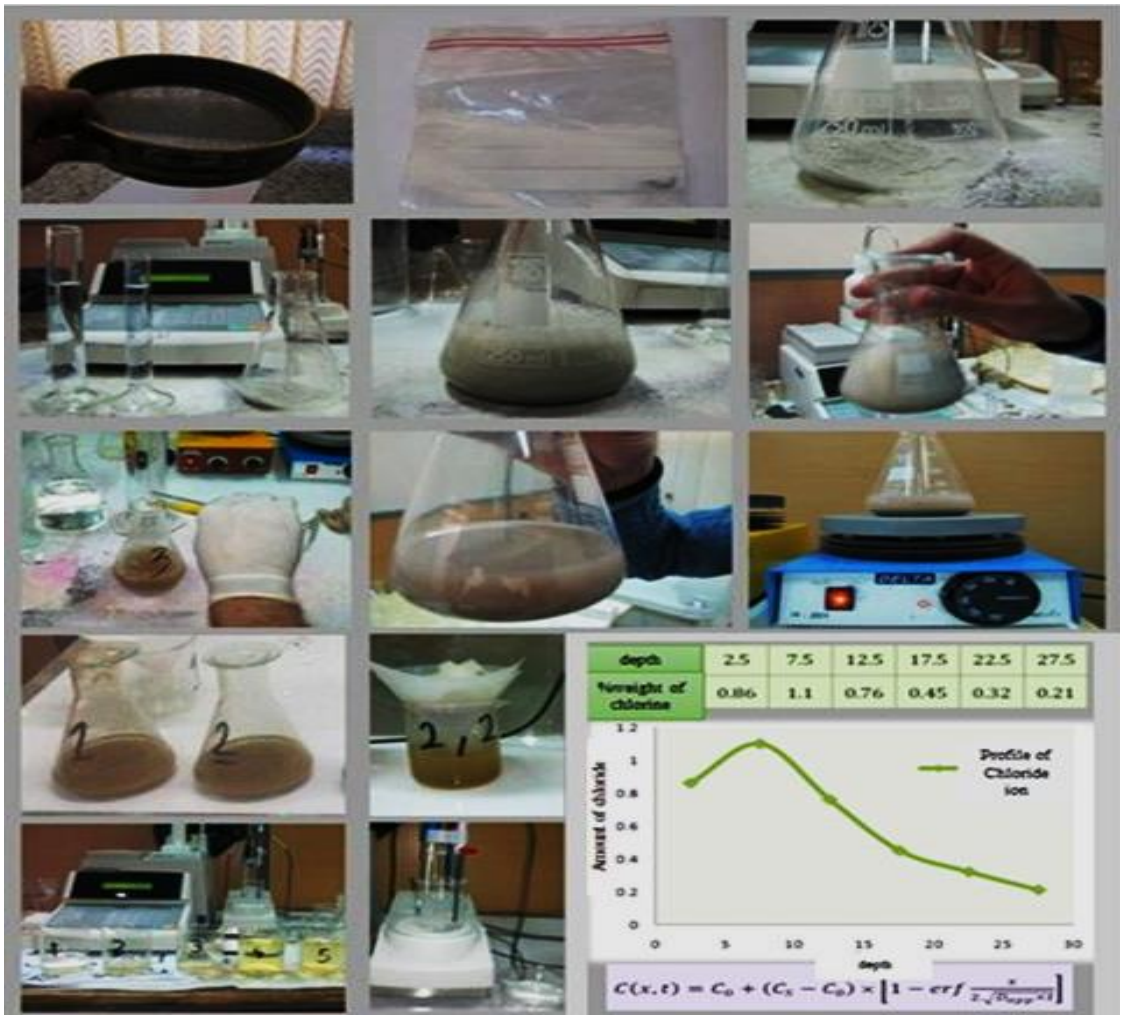

Fig. 4. A view of all the steps for preparing solutions according to ASTM C114 Standard (2017) and obtaining a chloride ion profile

Fig. 5. Measuring device electrical resistivity

The probable corrosion rate of concrete was determined on the basis of the electrical resistivity specified in Table 1, and in accordance with the recommendations of ACI 222 Standard (2001). It should be noted that the model of the device used in this test was Resipod Proceq, which also suggested the figures whereby the possible corrosion rate could be interpreted.

The standard method for performing the test in question is based on FM 5-578 FDOT (Ryan, 2011). Moreover, most electrical resistivity was performed together with half-cell potential tests in order to predict the possibility of corrosion. To perform this experiment according to the standard method, and also to eliminate the effect of reinforcement on the results, reading was performed in three directions at one point: horizontal, vertical and oblique. Considering the fact that the minimum cover in the members of the structure was not less than 30 mm, the effect of the armature on the test results is insignificant according to the explanations provided in the device catalog. As a result, the lowest number was reported as being the electrical resistivity. Similarly, information can be obtained about the concrete strength when it confronts aggressive factors from concrete electrical resistivity.

A concrete electrical resistivity test was performed at 23 points on the concrete Piers 11 and 12. The results are shown in Table 2. An outline of the results obtained by summarizing an electrical resistivity test for different elements of structure is shown in Table 3.

Table 1. Possible corrosion rates vs. Wenner test

Possible corrosion potential	Results of Wenner test (KΩ-cm)
Very high	5 >
High	5 - 10
Medium to low	10 - 20
Insignificant	20 <

Fig. 6. A view of the concrete superficial electrical resistivity test performed by using the Wener method on the concrete pier

Fig. 7. Concrete electrical resistivity test on Piles docks 11 and 12

Table 2. Test results for determination of concrete electrical resistivity

No	Test position	Test code	Moisture content	Vertical (kΩ/cm)	Horizontal (kΩ/cm)	Diagonal (kΩ/cm)
1	Wharf 11th Part 1.S	SR-P-01		65	62	67
2	Wharf 11th Part 1. A	SR-P-02		18	16	17
3	Wharf 11th Part 2. S	SR-P-03		33	34	39
4	Wharf 11th Part 2. A	SR-P-04		84	95	84
5	Wharf 31th Part 1.S	SR-P-05		97	150	167
6	Wharf 31th Part 1.A	SR-P-06	88%	307	327	300
7	Wharf 12th Part 5.S	SR-P-07		53	70	84
8	Wharf 12th Part 5.A	SR-P-08		66	94	98
9	Wharf 12th Part 6.N	SR-P-09		25	25	22
10	Wharf 12th Part 7.AN	SR-P-10		39	46	45
11	Wharf 12th Part 7.AS	SR-P-11		164	180	160

Table 3. Test results based on determining concrete electrical resistivity in the structure members

No	Structure element	Repair status	Minimum number read (KΩ-cm)	Maximum number read (KΩ-cm)	Possible corrosion rate (KΩ-cm)
1	Concrete piles	Repaired	13	73	Normal
2	Concrete piles	Non-repair	-	-	-
3	Structure concrete beams	Repaired	8	80	High
4	Structure Concrete beams	Non-repair section	15	88	Normal
5	Concrete slab under the pier	Repaired	23	38	Low
6	Concrete slab under the pier	Non-repair section	9	47	High
7	Forehead pier	Repaired	12	57	Normal
8	Forehead pier	Non-repair section	11	26	High

4.3. Pulse Velocity and Concrete Mechanical Modulus (Ultrasonic)

The ultrasonic pulse velocity technique performance was investigated (as a non-destructive test for concrete) to estimate the mechanical properties of concrete. The standard method used for this test was according to ASTM C597 (2002) and was performed to determine the pulse velocity of the concrete mechanical modulus, and it was non-destructive. This test is also known as ultrasonic pulse wave velocity, and is applied on the basis of determining the speed of these waves passing through the concrete. By the way, the most famous device used for this test is called Pundit. This device, which emits vibrations at its ordinary frequency, generates ultrasonic pulses by applying a sudden change of potential from an exciter transmitter to a piezoelectric transducer crystal. The transmitter transducer is in contact with the two sides of the concrete, and the vibrations caused in this way are received by it after passing through the concrete. In this test, it is possible to transmit generators in three

ways: direct, semi-direct and superficial. Of these three options, the first one is the most suitable for transmitting waves. Therefore, the variability of velocity along different paths in the structure is a sign of change in concrete quality. It is interesting to point out that pulse speed measurement can be used to control quality. It is also possible to establish an experimental relationship between pulse velocity and static and dynamic elasticity modulus and concrete strength. However, these relationships are influenced by factors such as the type and amount of cement, additives, aggregates, processing conditions and concrete age, as explained below:

$$V = \sqrt{\frac{(1-\mathrm{U})E_d}{p(1+\mathrm{U})(1-2\mathrm{U})}} \quad (5)$$

where V: is the pulse rate (m/s), υ: is the Poisson's ratio, p: is the concrete density (kg/m^3), and Ed: is the mechanical modulus of elasticity concrete (MN/m^2).

A concrete ultrasonic test was performed by using a Pundit Lap + device on different members of the structures at Piers 11 and 12. This experiment was performed to determine shear wave velocity in concrete, and to determine concrete mechanical elasticity modulus. Here, a concrete ultrasonic test was performed at 15 points of Piers 11 and 12. The results are shown in Figure 8 and Table 4.

A concrete qualitative classification using pulse velocity is shown in Table 5 (Maierhofer, 2010). The average quality of concrete in the beams is as follows: poor in piles, deck slabs, and pier forehead. The results of the concrete shear wave velocity test in different structure members are summarized in Table 6.

Table 4. Results of an ultrasonic concrete test (pulse velocity) on different members of Piers 11 and 12

Row	Test position	Test code	Test method	Shear wave velocity (m/s)	Quality category
1	Wharf 11th, south side of the pile on the axis B-31	UT-P-265	Indirect	2622	Weak
2	Wharf 11th, north side of the pile head on axis B-31	UT-CP-266	Indirect	2471	Weak
3	Wharf 11th, the lower side of the slab on axis 30th and 31th -A and B	UT-S-267	Indirect	2358	Weak
4	Wharf 11th, South face of the pile on axis B-11	UT-P-268	Indirect	2421	Weak
5	Wharf 11th, north side of the pile head on axis B-11	UT-CP-269	Indirect	2113	Weak
6	Wharf 11th - lower side of the slab on axis A and B-12 and 13	UT-S-270	Indirect	3318	Medium
7	Wharf 11th, west side of the beam on axis B and C-1	UT-B-271	Indirect	3563	Good
8	Wharf 11th, lower face of the slab on axis B and C-1 and 2	UT-P-272	Indirect	4518	Great
9	Wharf 12th, west side of the beam on axis B and C-1	UT-B-273	Indirect	2620	Weak
10	Wharf 12th, lower side of the slab on axis B and C-1 and 2	UT-S-274	Indirect	2439	Weak
11	Wharf 12th, south face of the pile head on axis B-1	UT-CP-275	Indirect	3764	Good
12	Wharf 12th, south side of the pile on axis B-2	UT-P-276	Indirect	2182	Weak
13	Wharf 12th, south face of the pile on axis B-11	UT-P-277	Indirect	2254	Weak

Table 5. Concrete quality classification based on pulse velocity

Concrete quality	Pulse speed	
	ft/s	m/s
Great	< 15	4500 >
Good	12 - 15	3500 - 4500
Medium	10 - 12	3000 - 3500
Weak	7 - 10	2000 - 3000
Very weak	7 <	2000 <

Fig. 8. Concrete ultrasonic test on piles, slabs and forehead at Piers 11th and 12th

Table 6. A summary of ultrasonic test results in the structure of different structure members of Piers 11 and 12

No.	Structure element	Average shear wave velocity (m/s)	Quality category
1	Concrete piles	2655	weak
2	Concrete structure beams	3707	good
3	Concrete slab under pier	2610	weak
4	Pier forehead	2695	weak

5. Materials and Methods

In this study, Portland cement was used to make specimens. In addition, a mixture of river-type sand and crushed-type gravel was prepared (with a specific weight of 2560 kg/m^3 2650 kg/m^3, respectively). A suitable aggregate was also prepared.

5.1. Mixing Ratios

Three super plasticizers within the range of 2%, 4% and 6% were used separately by considering three types of microsilica (5%, 10% and 15% with a grade of 400), and by selecting three water-to-cement ratios (34%, 40% and 45%). The objective was to achieve a suitable slump in different designs in conformity with the aim of this study, i.e. the application of microsilica in order to improve mechanical properties, to increase durability, and to reinforce concrete compressive strength in offshore piers. This was followed by making a control sample made and tested from a cement of a mixed grade. The number of concrete mixtures studied was referred to as M*S*W*, where M: indicates microsilica, S: represents superplasticizer, and W: stands for water-to-cement ratio. As can be seen from Tables 7-9, based on the granulations of three types of Shootar materials, the most suitable mixing design which agrees well with the specifications was selected. The design had the following ingredients: 1) Crushed gravel (12-25) mm, 30% by weight; 2) Broken gravel (5-19) mm, 30% by weight; 3) Natural washed sand (0-8), 40 mm by weight; 4) the mixing plan is done according to the specifications shown in Table 7; 5) Consumable cement is considered Type 2 from Tehran Cement Factory having a 400 kg per cubic meter grade; 6) The water cement ratio 0.34%, 0.40%, and 45% obtained with an average slump of 65 mm from Mahshahr Iran water. It must be pointed out that the mixing plan was drawn up on the basis of specifications seen in Table 7.

5.2. Cement Type

Durability of cement-based materials is an indication of their service life under a certain environmental conditions. Environmental conditions are the main factors in durability. According to ACI 201 (2008), durability of cement-based materials is their ability to withstand weathering, chemical attack, wear or any process which leads to damage (Tajdini et al., 2021). The consumable cement was considered to be of Type 2, Tehran Cement Factory, with a content of 400 kg per cubic meter. The cement chemical characteristics are given in Table 10.

Table 7. Concrete mix proportions

Mixing scheme number	W/C	SF (%)	Water (Kg/m^3)	Microsilica (Kg/m^3)	Cement (Kg/m^3)	Coarse-grained (Kg/m^3)	Fine-grained (Kg/m^3)
1	0.34	0	136	0	400	1118.4	745.6
2		5		20	380		
3		10		40	360		
4		15		60	340		
5	0.4	0	160	0	400	1104	736
6		5		20	380		
7		10		40	360		
8		15		60	340		
9	0.45	0	180	0	400	1092	728
10		5		20	380		
11		10		40	360		
12		15		60	340		

Table 8. Results of specific weight, dry volume unit weight and materials water absorption

Description	Appearance specific weight (gr/cm^3)	Real specific weight (gr/cm^3)	Dry volume unit weight (gr/cm^3)	Water absorption (%)
Gravel 12-25	2.710	2.645	1.39	0.86
Gravel 5-19	2.722	2.66	1.5	1.04
Sand 0-8	2.712	2.604	1.59	1.53

Table 9. Results of abrasion percentage using the Los Angeles and sand equivalence method

Description of specimens	Cycle drop	Abrasion weighing	Permissible limits of abrasion	Sand equivalence	Permissible limits of sand equivalence
Gravel 12-25 mm	500	17.6	40	--	--
Gravel 5-19 mm	500	21	40	--	--
Sand 0-8 mm	--	--	--	0.16	75

Table 10. Chemical characteristics of consumable cement

Chemical composition	SiO_2	Al_2O_3	SO_3	Fe_2O_3	CaO	MgO	C_3S	C_2S	C_3A
Percentage	21.97	4.26	1.65	3.55	64.56	2.33	50.68	24.76	3.65

5.3. Superplasticizer Additive

A concrete superplasticizer is a type of chemical additive with a water-reducing function. This reduction in water content will cause concrete strength and durability to increase. For purposes of this research, MECRET TB 101F was used, which is a delayed superplasticizer whose combined base includes naphthalene and melamine, and which is resistant to corrosion. As a result, it is suitable for offshore structures and corrosive environments.

Table 11. Chemical characteristics of consumable cement

Characteristic	Description
Appearance	Powder – brown
Volumetric weight	5507 gr/lit
PH of 20% solution	Approximately between 8 to 11

5.4. Microsilica

In this study, microsilica with a particle density of 2200 kg/m^3 was used. Table 12 presents the results of the chemical analysis of this microsilica.

5.5. Selection Criteria

Two standards, ASTM and ASTM C33 were used to make laboratory specimens and select materials. Based on the criteria of regulation, maximum grain size was used to make laboratory specimens (ASTM, 2021).

6. Results and Discussion

Cubic specimens in three dimensions (15 × 15 × 15 cm) were made to evaluate the compressive strength of concrete, and to conduct an analysis of each specimen with a view to measuring compressive strength and corrosion current density. The specimens were submerged to the sea water in order to test them for corrosion. The results of the compressive strength experiment are shown in Table 14.

Table 12. Chemical properties of microsilica

Chemical composition	SiO_2	Al_2O_3	Fe_2O_3	CaO	MgO	SO_3
Percentage	95.1	1.32	0.87	0.49	0.97	0.1

Table 13. Determining the percentage of ingredients in concrete laboratory specimens

Sample code	**W/C**	**Type of cement**	**Microsilica (%)**	**Superplasticizer (%)**
M0S6w34:1	34%	2	0	0.6
M5S6w34:2			5	
M10S6w34:3			10	
M15S6w34:4			15	
M0S2w40:5	40%		0	0.4
M5S2w40:6			5	
M10S2w40:7			10	
M15S2w40:8			15	
M0S2w45:9	45%		0	0.2
M5S2w45:10			5	
M10S2w45:11			10	

Table 14. The results of compressive strength tests on concrete specimens for 28 days

Specimen code	**Length (cm)**	**Width (cm)**	**Height (cm)**	**Maximum force (kg)**	**Compressive strength (kg/cm^2)**
M0S6w34:1	15.1	15.1	15	126800	383
M5S6w34:2	15.1	15	15	152160	579
M10S6w34:3	15.2	15.2	15.3	158500	603
M15S6w34:4	15.1	15.1	15.1	164840	627
M0S2w40:5	15.1	15.1	15.1	121600	365
M5S2w40:6	15.1	15	15	148300	534
M10S2w40:7	15.2	15.1	15.1	153400	581
M15S2w40:8	15.1	15	15	157600	590
M0S2w45:9	15.1	15.1	15	111500	321
M5S2w45:10	15.1	15	15	124820	484
M10S2w45:11	15.3	15.1	15.1	134700	505
M15S2w45:12	15.1	15	15	148800	558

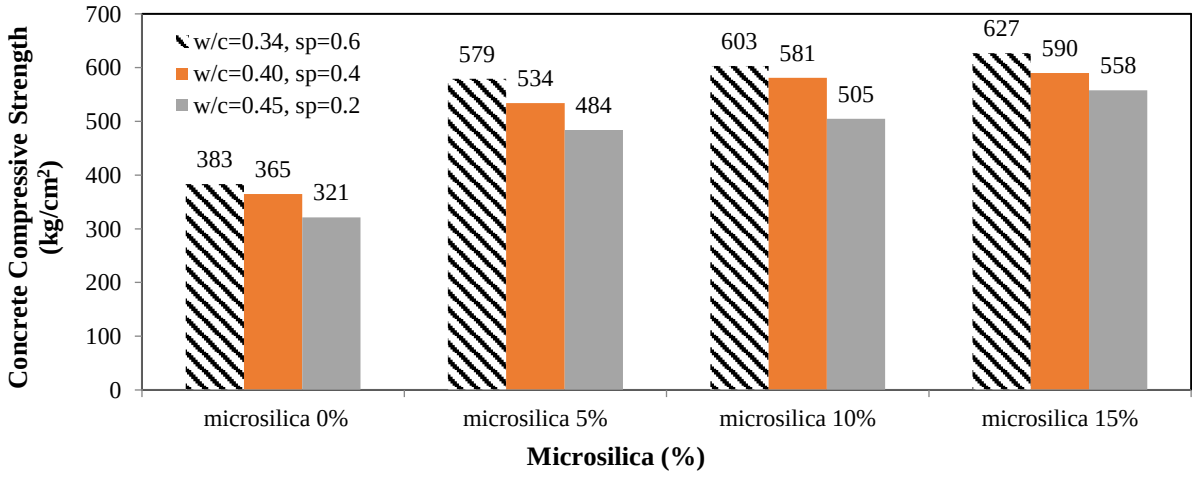

Fig. 9. The effect of microsilica on concrete compressive strength for 28 days

Table 15. Ranges of corrosion current density and their interpretation (Gu et al., 2000)

Extent of corrosion	**Corrosion current density ($\mu A/cm^2$)**
Passive condition	$icorr < 0.1$
Low to moderate corrosion	$0.1 < icorr < 0.5$
Moderate to high corrosion	$0.5 < icorr < 1$
High corrosion	$icorr > 1$

In this study, concrete specimens were kept in a laboratory in the Persian Gulf environment for 18 months. Corrosion tests were then conducted on the laboratory samples 80 times for 4.5 months, and the test results were compared with each other.

The results are shown in Figures 10-12. In Figure 10, the effect of microsilica on the compressive strength of concrete for 28 days, with three water-to- cement ratios and 3% superplasticizer are shown. It can be seen from the figure that the average compressive strength increases by 30%, compared with the control specimen without microsilica, thus reducing the ratio of water to cement, as well as the use of microsilica. In these figures, the corrosion current density is presented, in terms of the age of concrete (i.e., corrosion duration), for specimens containing microsilica 15%, 10%, and 5% (weight of cement), and for those without microsilica. This involves Type 2 cement. After 18 months, the corrosion current density within the range of 5%,10%, and15% was less than that of the specimen without microsilica (see Figures 11 and 12). The fineness of the microsilica grains, compared with the round grains of cement, can be said to be the reason for this decrease. First, they fill very fine spaces of glaze when they are placed next to the cement glaze. Secondly, they combine with calcium hydroxide [$(OH)_2$] resulting from the dewatering of the cement and convert it into hydrated calcium silicate because they are chemically active. In this way, voids are reduced in the cement glaze, the calcium hydroxide changes into a more solid body (similar to other cement paste silicates), the cement paste texture becomes more uniform, and the concrete properties are improved. In all three figures, the corrosion current density is shown on the basis of the age of concrete with three water-to-cement ratios (0.34%, 40%, and 45%) and by considering 3 percentages of different microsilica. These figures show that the corrosion current density within the range of 10% and 15% is much lower than that of samples without microsilica and the instances of corrosion intensities are very close to each other. It can be observed that the difference between the corrosion current density of mixtures containing 10% microsilica, and that of mixtures containing 15% microsilica, arises from an increase in calcium hydroxide, which itself results from the hydration of cement and water in higher grade mixtures. As a result, when there are higher amounts of microsilica, they increase the gel and neutralize the negative effect of the excess mixture. Although the ratio of microsilica is 15% lower than the other two ratios of it, because of the trend of severe corrosion in shapes, it can be seen from these figures that the two ratios of microsilica (i.e., 10% and 15%) are very close to each other and the important factor at this stage is the economics of microsilica consumption, as indicated by its large volume in this project.

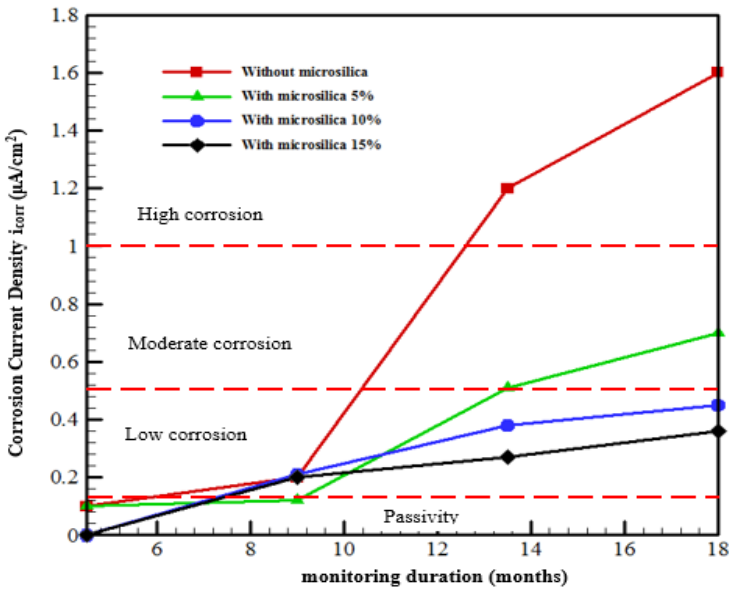

Fig. 10. Corrosion rate of concrete specimens at different times (SP = 0.6, w/c = 0.34)

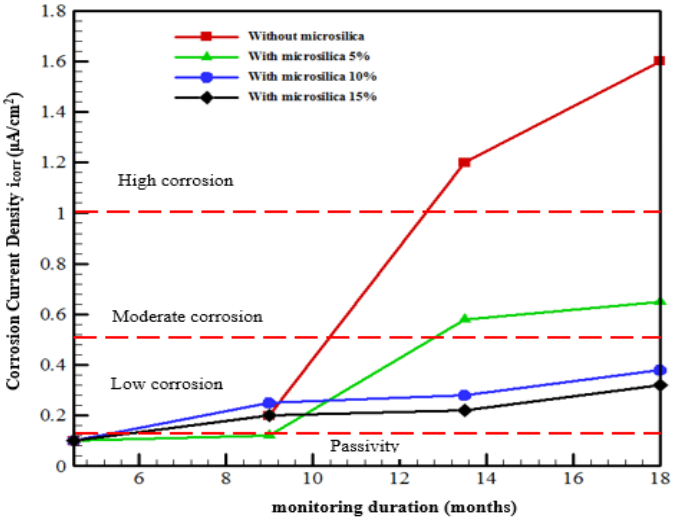

Fig. 11. Corrosion rate of concrete specimens at different times (SP = 0.4, w/c = 0.40)

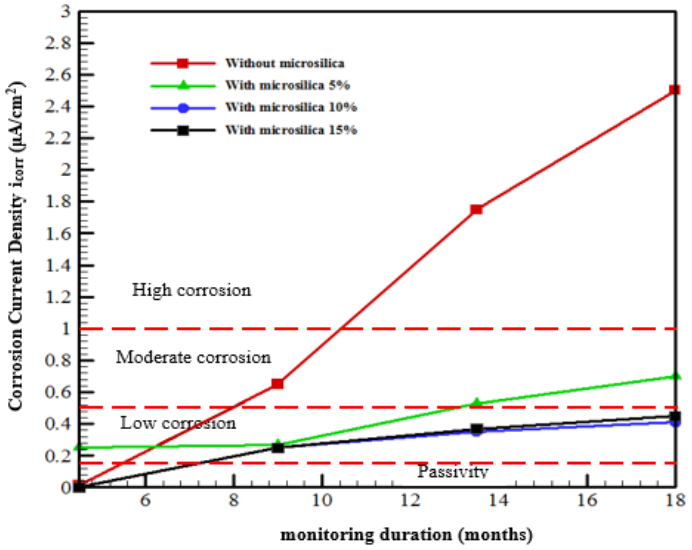

Fig. 12. Corrosion rate of concrete specimens at different times (SP = 0.2, w/c = 0.45)

7. Conclusions

The results demonstrated that the number of invasive salts in the Persian Gulf water is significantly higher than the average quantity determined for open seas. This high concentration in seawater results mostly from high evaporation of water, low rainfall, and the presence of polluting petrochemical industries in the region. From the results, it is indicated that over time, concrete piles have suffered the most damage because of chloride penetration and reinforcement corrosion and, therefore, must be repaired by using appropriate materials. The tidal zone is an area subject to changes at water level and constantly becomes wet and dry so that most destruction of the concrete takes place. Given that the corrosion of rebar's is one of the main factors in destroying reinforced concrete structures, concrete permeability is the most important cause of the increasing rate of this destruction. In this connection, the use of pozzolanic materials such as microsilica plays a significant role to have a dense concrete and increasing electrical resistivity at concrete and reducing the permeability of concrete. On the basis of the results obtained from this study it is suggested that the microsilica used in concrete should be about 10%. Because of the reduction of concrete permeability, it is suggested that the water-to-cement ratio and superplasticizer should be 34% and 6%, respectively.

8. Acknowledgement

The authors are grateful to the Imam Khomeini Port managers for providing facilities where part of this work was carried out.

9. References

Abedini, M. and Zhang, C. (2021). "Dynamic vulnerability assessment and damage prediction of RC columns subjected to severe impulsive loading", *Structural Engineering and Mechanics*, 77(4), 441.

ACI 201. (2008). *Guide to durable concrete*, American Concrete Institute.

ACI 222 Standard. (2001). *Protection of metals in concrete against corrosion*, American Concrete Institute.

Antunes, D., Martins, R., Carmo, R., Costa, H. and Júlio, E. (2021). "A solution with low-cement light weight concrete and high durability for applications in prefabrication", *Construction and Building Materials*, 275, 122153.

ASTM C597. (2002). *Standard test method for pulse velocity through concrete*, ASTM International.

ASTM C114. (2017). *Chemical Analysis of Hydraulic Cement*, ASTM International.

ASTM. (2021). *Standard specification for concrete aggregates, Annual Book of ASTM Standards*, 04.02, USA.

Babaee, M. and Castel, A. (2016). "Chloride-induced corrosion of reinforcement in low-calcium fly ash-based geopolymer concrete", *Cement and Concrete Research*, 88, 96-107.

Babaee, M. and Castel, A. (2018). "Chloride diffusivity, chloride threshold, and corrosion initiation in reinforced alkali-activated mortars: Role of calcium, alkali, and silicate content", *Cement and Concrete Research*, 111, 56-71.

Bagheri, A., Zanganeh, H., Alizadeh, H., Shakerinia, M. and Marian, M.A.S. (2013). "Comparing the performance of fine fly ash and silica fume in enhancing the properties of concretes containing fly ash", *Construction and Building Materials*, 47, 1402-1408.

Baqheri, A.R., Zanganeh, H., Samadzad, H. and Kiani, A.L.A.H. (2012). "Assessing the durability of binary and ternary concretes using rapid chloride resistance test and the accelerarted rebar corrosion test", *The International Congress on Durability of Concrete*, Tehran, Iran.

Ganjian, E. and Pouya, H.S. (2009). "The effect of Persian Gulf tidal zone exposure on durability of mixes containing silica fume and blast furnace slag", *Construction and Building Materials*, 23(2), 644-652.

Gu, P., Beaudoin, J., Zhang, M.H. and Malhotra, V. (2000). "Performance of reinforcing steel in concrete containing silica fume and blast-furnace slag ponded with sodium-chloride solution", *Materials Journal*, 97(3), 254-262.

He, B., Gao, Y., Qu, L., Duan, K., Zhou, W. and Pei, G. (2019)."Characteristics analysis of self-luminescent cement-based composite materials with self-cleaning effect", *Journal of Cleaner Production*, 225, 1169-1183.

He, X., Zheng, Z., Yang, J., Su, Y., Wang, T. and Strnadel, B. (2020). "Feasibility of incorporating autoclaved aerated concrete waste for cement replacement in sustainable building materials", *Journal of Cleaner Production*, 250, 119455.

Liu, J., Huang, H., Ma, Z.J. and Chen, J. (2021). "Effect of shear reinforcement corrosion on interface shear transfer between concretes cast at different times", *Engineering Structures*, 232, 111872.

Li, C.Q. and Zheng, J.J. (2005). "Propagation of reinforcement corrosion in concrete and its effects on structural deterioration", *Magazine of Concrete Research*, 57(5), 261-271.

Parrott, L. (1994). "A study of carbonation-induced corrosion", *Magazine of Concrete Research*, 46(166), 23-28.

Moffatt, E. and Thomas, M. (2018). "Performance of 25-year-old silica fume and fly ash lightweight concrete blocks in a harsh marine environment", *Cement and Concrete Research*, 113, 65-73.

Maierhofer, C., Reinhardt, H.W. and Dobmann, G. (2010). *Non-destructive evaluation of reinforced concrete structures: Non-destructive testing methods*, Woodhead Publishing.

Poston, R.W., Kesner, K., McDonald, J.E., Vaysburd, A.M. and Emmons, P.H. (2001). "Concrete repair material performance, Laboratory study", *Materials Journal*, 98(2), 137-147.

Pandey, A. and Kumar, B. (2019). "Evaluation of water absorption and chloride ion penetration of rice straw ash and microsilica admixed pavement quality concrete", *Heliyon*, 5(8), e02258.

Roy, S., Poh, K. and Northwood, D. (1999). "Durability of concrete accelerated carbonation and weathering studies", *Building and Environment*, 34 (5), 597-606.

Ryan, E.W. (2011). "Comparison of two methods for the assessment of chloride ion penetration in concrete: A field study", M.Sc. Thesis, University of Tennessee.

Siddique, R. (2011). "Utilization of silica fume in concrete: Review of hardened properties", *Resources, Conservation and Recycling*, 55(11), 923-932.

Tajdini, M., Bargi, M.M. and Rasouli Ghahroudi, O. (2021). "An investigation on the effects of adding nano-sio_2 particles and silica Ffume with different specific surface areas on the physical and mechanical parameters of soil-cement materials", *Civil Engineering Infrastructures*

Journal, 54(1), 93-109.
Zhang, C., Abedini, M. and Mehrmashhadi, J. (2020). "Development of pressure-impulse models and residual capacity assessment of RC columns using high fidelity Arbitrary Lagrangian-Eulerian simulation", *Engineering Structures*, 224, 111219.
Zhang, C. and Abedini, M. (2021), "Time-history blast response and failure mechanism of RC columns using Lagrangian formulation", *Structures*, Elsevier, 34, 3087-3098.